

# Complexity Measures of Event Related Potential Surface Laplacian Data Calculated Using the Wavelet Packet Transform

Kevin Jones\*, Henri Begleiter\*, Bernice Porjesz\*, Kongming Wang\*, and David Chorlian\*

**Summary:** We describe a method to obtain estimates of EEG signal complexity using the well-established wavelet packet transform with best basis selection. In particular, we use the two-dimensional wavelet packet transform to obtain estimates of the complexity of two-dimensional images. This allows us to calculate complexity estimates of high-resolution brain potential maps generated from 61 scalp electrode Visual Oddball paradigm, grand-mean data. A significant reduction in the complexity of the surface Laplacian time-slices is observed during and after the Visual Potential 300 (P3) event for the target case, possibly as a result of increased spatial synchrony associated with visual-related tasks. We also present the results of a statistical analysis of the largest principal component of the time-varying complexity curves, for control, high-risk, and alcoholic groups of male subjects. Parametric and non-parametric analyses show differences in the complexity data which are significant between the control group and the alcoholic and high-risk groups.

**Key words:** ERP; Brain's electrical fields; Surface Laplacian; Wavelet packet transform; Complexity; Entropy.

## Introduction

Traditionally, the amplitude and frequency content of electroencephalogram (EEG) and event related potential (ERP) signals are employed to examine differences between experimental cases or population groups. Temporal and spatial measures of signal entropy (or complexity) offer an alternative method to analyze neurophysiological signals as they use a measure that is less sensitive to possible differences in absolute signal measures such as amplitude and frequency. Fell et al. (1996) showed that a number of other linear and non-linear measures, such as correlation dimension, Lyapunov exponents and entropy, offered additional complementary information to that of spectral measures for the discrimination of sleep stages using EEG data. Rezek and Roberts (1996) argue that EEG rhythms may be manifestations of changes in the interaction be-

tween neuronal assemblages; hence, measures of signal entropy could provide a useful alternate method of analysis. A number of recent articles (Pezard et al. 1996; Roberts et al. 1998; Weber et al. 1998; Andino et al. 2000; Bhattacharya 2000; Bergey and Franaszczuk 2001; Jeong et al. 2001) have described the application of entropy and complexity measures to EEG and ERP data in order to differentiate cognitive tasks or clinical groups.

Here we apply a measure of signal complexity to high-resolution ERP data collected during a simple discrimination task "oddball" paradigm. This complexity measure is based on the concept of Shannon entropy (Shannon 1948), historically the first measure of signal randomness or disorder. The term "entropy" here refers to the analogy between the Shannon entropy formula and the equation for thermodynamic entropy. The entropy of a sequence has a number of equivalent interpretations:

\* Entropy is a measure of the complexity of the random process that generates the sequence, where larger entropy values represent higher process uncertainty and therefore higher complexity.

\* Entropy is the length of shortest binary description of the states of the random variable that generates the sequence, so it is the size of the most compressed description of the sequence.

\* Entropy also measures the average surprise, or information gain, occasioned by the receipt of a symbol.

Shannon entropy is considered a standard measure of the complexity of a sequence (Lloyd 1989), and is

\* Neurodynamics Laboratory, Department of Psychiatry, SUNY Health Science Center at Brooklyn, Brooklyn, NY, USA.

Accepted for publication: April 5, 2002.

The authors would like to thank Edward Babington, Howard Cohen, Debra Josephson, Stacie Richardson, Aquanette Sass, Arthur Stimus and Alyson Wahl for their valuable technical support. This research is supported by N.I.H. grant AA 12560.

Correspondence and reprint requests should be addressed to Dr. Kevin Jones, Neurodynamics Laboratory, Department of Psychiatry, SUNY Health Science Center at Brooklyn, 450 Clarkson Avenue, Brooklyn, NY, USA, 11203.

Copyright © 2002 Human Sciences Press, Inc.

closely related to Kolmogorov's algorithmic complexity measure - defined as the length of the shortest program for a universal Turing machine that correctly reproduces the observed data (Kolmogorov 1965). The Shannon entropy of a random variable  $X$  is:

$$H[X] \equiv - \sum_{x \in \chi} \Pr(x) \log_2(\Pr(x)), \quad (1)$$

where  $H[X]$  is a function of the probability distribution of the random variable  $X$ .

Recently, a number of alternatives have been devised to determine the information content of a signal. These include: Rényi entropy (Rényi 1960); correlation dimension (Grassberger and Procaccia 1983); Lyapunov exponent (Wolf et al. 1985); Taken's maximum likelihood estimator (Takens 1981); approximate entropy (Pincus 1991); spectral entropy and embedding-space decomposition (Rezek and Roberts 1996); Time-frequency representation Rényi entropy (Baraniuk et al. 1998). These linear and non-linear measures quantify signal complexity; however, the technical definitions of "complexity" vary according to the method.

## Methodology

In this paper we apply a method to calculate the complexity of ERP time slice images using the two-dimensional wavelet packet decomposition (Coifman and Wickerhauser 1990) with best-basis selection (Coifman and Wickerhauser 1992). This provides an estimate of spatial entropy at successive time points. Use of the wavelet packet best-basis coefficient as a measure of signal complexity has, to the authors knowledge, not been reported elsewhere, and hence represents a new and novel method of analyzing spatial ERP data. We show the application of the measure to high-resolution Visual Oddball data.

Significant differences are observed between control vs. alcoholic and control vs. high-risk spatial complexities during and following the Visual P3 component for the target stimulus case of the Visual Oddball experiment. The Visual P3 component is the third positive component of the ERP; it occurs between 300 and 500 ms after the stimulus onset. Differences in the Visual P3 component amplitude between control and alcoholic men have been reported on several occasions (Porjesz et al. 1980, 1987; Emmerson et al. 1987; Patterson et al. 1987; Pfefferbaum et al. 1991; Cohen et al. 1995). In all these studies, the primary finding is a decrease in the Visual P3 component amplitude of the ERP in abstinent alcoholics compared with controls. Similar observations have been made between low-risk and high-risk boys (Begleiter et al. 1984; Benegal et al. 1995; Whipple et al. 1988, 1991; Berman et al. 1993; Hill et al. 1993; van der Stelt et al. 1998).

The differences between the groups presented in this paper, however, are independent of Visual P3 component peak amplitude measures and so possibly represent a different putative phenotypic marker for the study of the genetic predisposition toward alcoholism.

## Materials and Methods

### Measuring Data Complexity

Sparse coding provides a way to determine the complexity of a signal or image. A signal which is maximally sparse will have a probability distribution which is highly peaked around zero and which contain significant tails, e.g., figure 1a. Such highly peaked probability distributions describe low entropy signals in which most values will be zero and where there is a reduction of statistical dependency among the signal coefficients (Olshausen and Field 1996). In contrast, a Gaussian distribution with the same variance will have maximal entropy. Sparse coding can be achieved through a variety of compression algorithms, and a measure of complexity can be obtained using some measure of the effectiveness of the compression algorithm (illustrated in figure 1b).

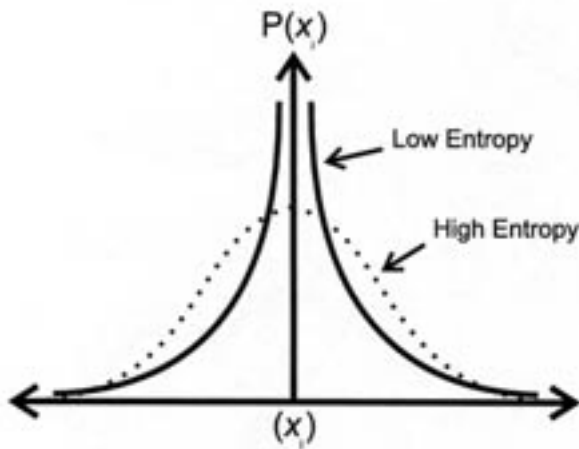
The Coifman and Wickerhauser (1992) best-basis algorithm is used here to determine a transformation which yields the best compression for the wavelet packet transform (Coifman and Wickerhauser 1990). The best-basis algorithm can deliver near-optimal sparsity representations of a signal. The next section gives a brief outline of the techniques employed to deliver an estimate of signal complexity: the wavelet packet transform decomposition and best-basis.

### Wavelet packet transform, best-basis, and signal complexity

The wavelet packet transform is a generalization of the wavelet transform, which decomposes a signal  $f(t)$  into a weighted sum of basis functions. The basis functions are translated and dilated versions of a mother wavelet function  $\psi$ , which define the orthogonal wavelet basis, and is formed using the two fundamental equations upon which the wavelet calculations are based, the scaling function  $\phi$  and wavelet function  $\psi$ .

The wavelet packet transform generates the full decomposition tree, as depicted in figure 2; this is an overdetermined system (if  $*f^* = 2^n$  then each row in the decomposition tree has  $2^n$  coefficients and the wavelet packet tree has  $n2^n$  coefficients). A particular choice of subtree coefficients which represent a signal using the same number of samples as the original is termed a basis. For example, the coefficient sets depicted by white ovals in figure 2 represent one possible basis representation of

(a) Probability Distribution



(b) Sparse Representation

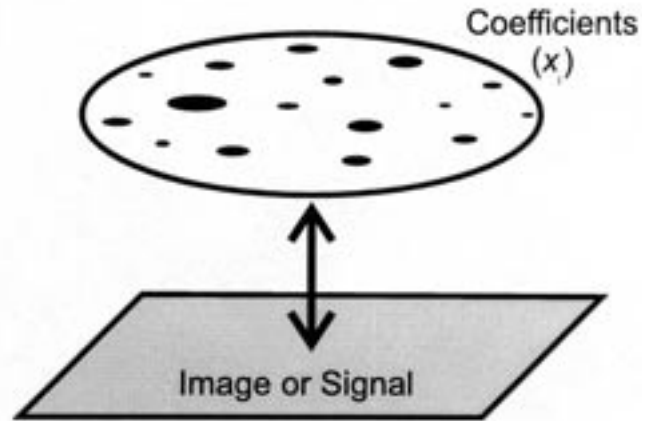


Figure 1. A highly peaked distribution with heavy tails, solid line in (a), will have low entropy and hence reduced statistical dependencies among coefficients. In contrast, a Gaussian distribution (dotted line in (a)) has maximum entropy for the same variance. Sparse coding of an image or signal, depicted in (b), provides transformation of the data to a lower entropy form. Figure adapted from Olshausen and Field (1996).

the signal  $f$ . (Wavelet transform coefficients are depicted in figure 2 with gray ovals.) Commonly, the lowest cost basis with respect to a cost function is chosen to represent the signal. Typically employed cost functions include:  $L^p$  norm (where  $p$  is some positive integer);  $L^2$  entropy; and counting of the number of elements above a threshold value (Coifman and Wickerhauser 1992).

Trgo and Wickerhauser (1996) show how the best-basis algorithm of Coifman and Wickerhauser (1992) can also provide an estimate of the signal compression rate, since the best-basis algorithm minimizes the theoretical dimension of a sequence. This estimate is related to Shannon-Weaver entropy, the minimum bit rate required to transmit the values of the signal (Shan-

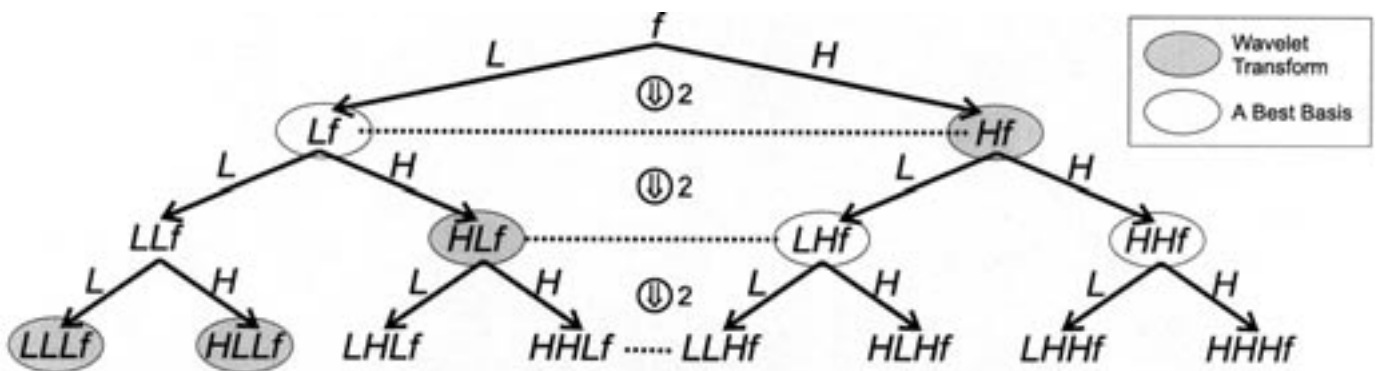


Figure 2. Illustration of the wavelet packet decomposition. A low ( $L$ ) and high ( $H$ ) pass filter is repeatedly applied to the function  $f$ , followed by decimation by 2, to produce a complete subband tree decomposition to some desired depth. The low- and high-pass filters are generated using orthogonal basis functions. The wavelet transform basis is indicated by gray ovals. The orthogonality of the basis functions allows the use of an additive cost function to determine the optimal basis for data compression. An example of a possible best basis is shown using white ovals.

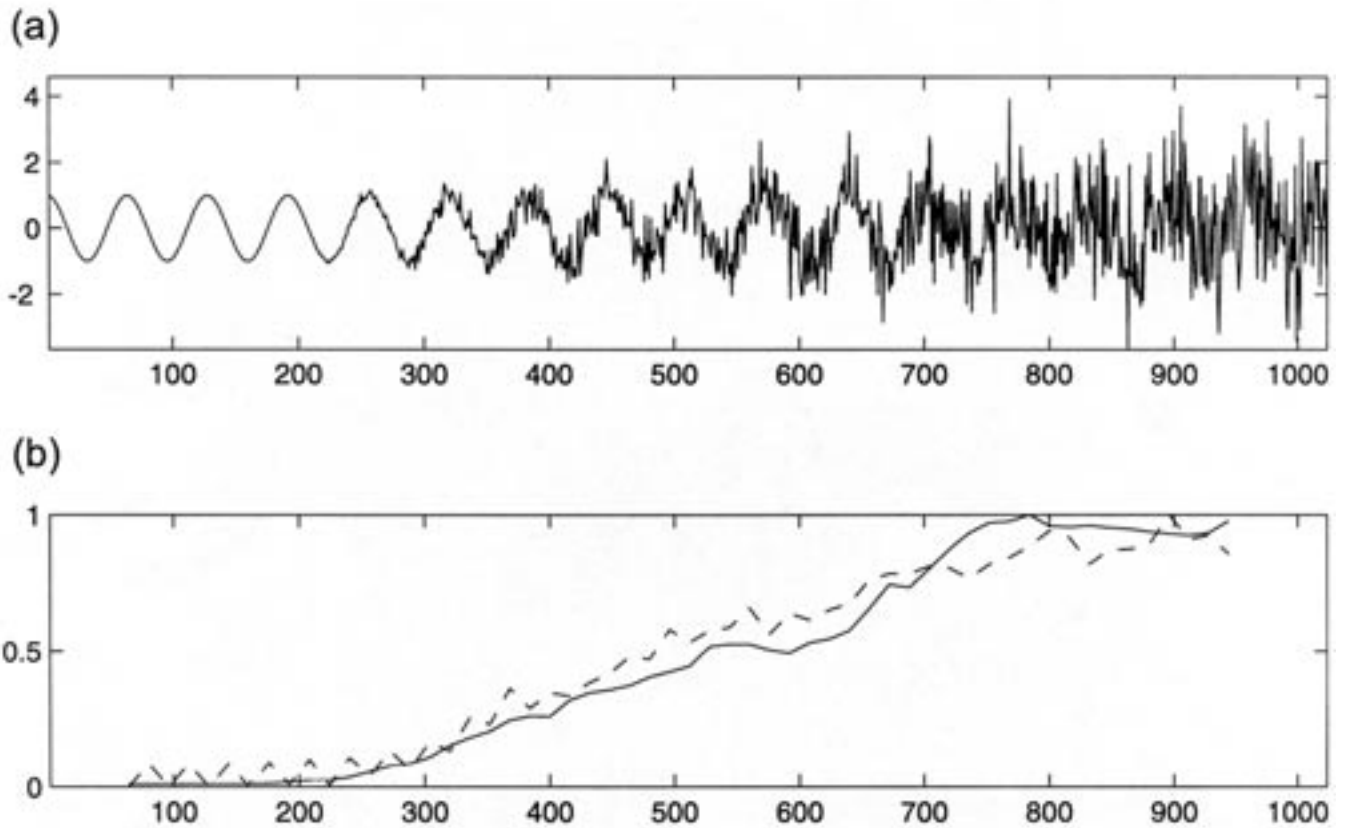


Figure 3. One-dimensional complexity calculation example for a deteriorating sinusoid (a). Sliding window complexity values are shown in (b) calculated using the one-dimensional wavelet packet decomposition and the best-basis algorithm (solid line) and Rényi entropy estimation via time-frequency representations (dashed line) (Baraniuk et al. 1998; Andino et al. 2000). Both complexity measures employed a 128 sample sliding window with 16 samples overlap. Entropy and complexity curves have been amplitude normalized to allow comparison.

non and Weaver 1964). In this study the value of the  $L^2$  norm cost function for the best basis is used as a measure of the effectiveness of the compression algorithm, and hence as a measure of the relative complexity of a signal or image. Additionally, all complexity calculations use the symmlet wavelet with eight vanishing moments as a basis function for wavelet decompositions. As an example, figure 3 shows complexity estimates for a 1024 point sinusoidal signal  $x(t)$ , with increasing amplitude additive noise (figure 3a). Two complexity measures are plotted in 3b: signal complexity, calculated via wavelet packets and best-basis; and the Rényi entropy, calculated via time-frequency representations (following Baraniuk et al. 1998 and Andino et al. 2000). Both measures show the same general behavior - signal complexity increasing with increasing additive random noise.

Extension of the wavelet packet transform to analyze two-dimensional signals is described by Coifman and Meyer (1990). If  $\psi$  is the mother wavelet and  $\phi$  the

scaling function, then the two-dimensional basis is given by the functions

$$\begin{aligned} &\phi_{(j,k)}(x)\phi_{(j,k')}(y), \\ &\psi_{(j,k)}(x)\phi_{(j,k')}(y), \\ &\phi_{(j,k)}(x)\psi_{(j,k')}(y), \end{aligned}$$

The best basis tree is chosen using a cost function calculation on each sub-matrix of the decomposition in an analogous way to the one-dimensional case (figure 2). The final relative complexity value of the image is then equal to best overall cost-function value.

Figure 4 shows synthetic checkerboard images with either 4 (a, b and c), 16 (d, e and f) or 64 (g, h and i) squares and increasing SNR (Gaussian noise) of 4 (a, d and g), 10 (b, e and h) and 2 (c, f and i). The signal-to-noise ratio (SNR) is here defined as the magnitude of the signal (the same for all check patterns) divided by the mean abso-

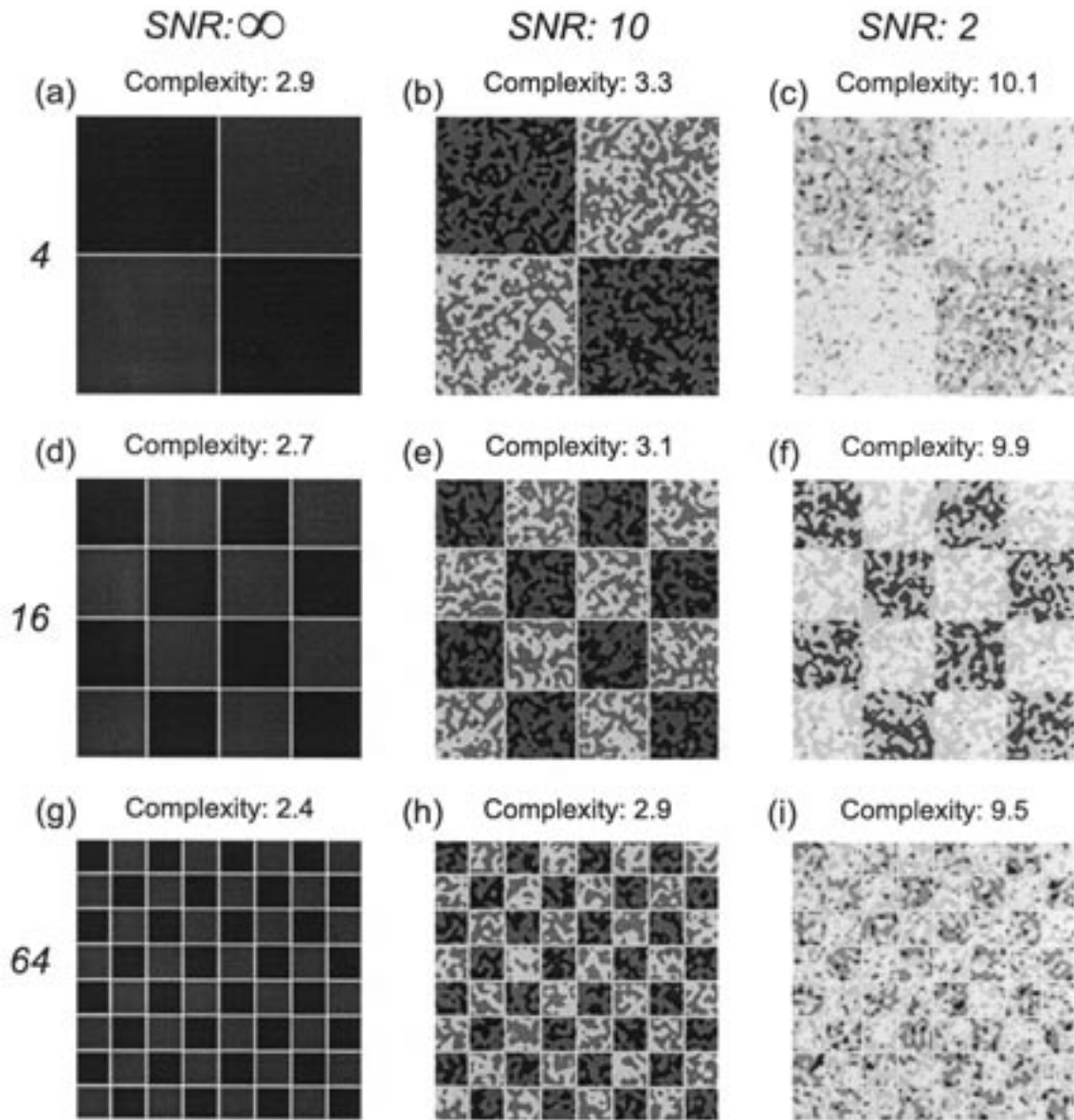


Figure 4. Two-dimensional complexity calculation examples for checkerboard images with additive Gaussian noise. Checkerboard images have 4 (a, b and c), 16 (d, e and f), or 64 (g, h and i) checks; and signal to noise ratios (SNR) of 4 (a, d and g), 10 (b, e and h), or 2 (c, f and i).

lute noise level (infinite SNR is therefore noise free). As might be expected the images containing greater noise show higher relative complexity values. Somewhat counter-intuitively, however, images with a larger number of checks show lower complexity values. This effect may be understood through the notion of average surprise (Feldman 1998), which is related to the degree of uncertainty. The quantity  $-\log_2 \Pr(x)$  in the Shannon entropy equation (equation 1) may be referred to as the surprise associated with the outcome  $x$ , and is large when  $\Pr(x)$  is small. The landscape depicted in the image with

64 squares (figure 4c) is more predictable, and hence will contain less surprise, than the landscape with 4 squares (figure 4g). It is interesting to note that images figure 4a and 4h have similar complexity values despite their different nature, i.e., the measure is non-unique.

#### The Visual Oddball Paradigm Experiment Data

##### Data collection

During the Visual Oddball experiment the subject is seated in a dimly lit, temperature regulated, sound atten-

uated booth (Industrial Acoustics Corp., Bronx, NY). Data were recorded using a 64 channel electrode cap (Electro Cap Intl., Inc., Eaton, OH), 61 placed using the International 10/20 system (Jasper 1958), 2 channels monitoring eye movement and 1 nose channel acting as a reference channel. EEG activity was amplified 10 K (Sensorium, Charlotte, VT), and bandpassed at 0.02 - 50 Hz, before being digitally sampled and recorded at a rate of 256 Hz. Subjects were requested to sit as still as possible and minimize blinking during data recording.

The Visual Oddball paradigm consists of 280 stimuli separated by a uniform inter-stimulus interval of 1.625 seconds and presented for 60 ms duration. Of the 280 stimuli, 210 are non-targets represented by the outline of a square, 35 are target stimuli in the shape of a cross, and 35 are novel, formed from differing geometrical shapes; the subjects are instructed to respond to the target stimulus by pressing a button as quickly as possible. Speed was emphasized but not at the expense of accuracy. The stimuli were presented in a pseudo-random order with the constraint that the targets or novels may not be repeated consecutively.

Following acquisition, the data were separated into trials with 200 ms of pre-stimulus baseline data and 800 ms post-stimulus data, and then grouped into the three cases. An artifact threshold level of 75 microvolts was used to reject trials with eye and movement artifacts; consequently, the number of trials per case varies for different subjects. Commonly, the trials at this stage are filtered, averaged within target, non-target and novel cases (correct trials only), and analyzed using amplitude or frequency measures.

#### Data manipulation and complexity calculation

The Visual Oddball data were filtered with a low-pass filter of 32 Hz, followed by downsampling from 4 ms to 16 ms sample interval. This reduced the required data by a factor of four. Trial data which passed the threshold level test were then averaged according to target, non-target, and novel stimuli cases for each subject. In order to evaluate the temporal variations of the relative complexity of the spatial ERP pattern, the surface Laplacian was calculated from the average data following the algorithm described in Wang and Begleiter (1999). A spherical scalp is assumed for the convenience of the computations. The surface Laplacian of the data is calculated to provide high-resolution data (Nunez 1995), give a reference-independent estimate of the radial current source density (Katznelson 1981; Le et al. 1994; Nunez et al. 1994), and reduce the effects of electric field volume conduction through the head (Srinivasan et al. 1998). The surface Laplacian method employed here consists of a local surface approximation using a tangent plane followed by polynomial fitting; the coefficients were estimated by a

least-squares solution to a minimization problem (Wang and Begleiter 1999).

The two-dimensional wavelet packet transform is constructed in  $\mathbf{R}^n$  where  $n = 2$  (square). Therefore, in order to obtain the measurement of spatial complexity, the ERP data are required in a regular domain for the complexity measure. The half-sphere scalp surface may be transformed to a two-dimensional circle without distortion, which is then transformed to a square, with slight distortion, using the one-to-one mapping transformation described in Wang et al. (1998) and given in the Appendix. Figure 5 depicts the transformation of 61 electrodes and corresponding surface Laplacian data from a two-dimensional circle to a two-dimensional square. Note, the outer edge of data associated with peripheral electrode sites is discarded due to edge distortions caused by the surface Laplacian calculation.

The resulting data cube consists of 62 slices, corresponding to 1 second of data, for each of the three stimulus cases (200 ms pre stimulus data and 800 ms post stimulus data) per subject. Each slice is extracted from the data cube, amplitude normalized, and transformed using the two-dimensional wavelet packet best basis algorithm. The relative complexity value (value of the best basis cost function) is plotted as a function of time.

## Results

Figure 6 illustrates application of the method to a group of 45 male control subjects. Figure 6a shows a grand-average slice of the surface Laplacian at approximately 450 ms following the onset of the target stimulus. Figure 6b depicts the best basis wavelet packet transform coefficients with phase-planes overlaid for the selected basis. Figure 6c is a plot of the averaged complexity values over time (stimulus onset is at zero seconds); and for comparison the average brain potential at electrode CZ (mid-central electrode) is plotted in figure 6d. The main feature of the complexity curve is that both during and after the Visual P3 component (300 - 700 ms) there is a decrease in complexity, from values in the 3.5 - 5 range to a minimum value of less than 2. We suggest that this decrease may be the result of spatial synchronization of neuronal activity associated with the Visual P3 response for the target case. For the novel and non-target case data a decrease in the complexity value is also observed during the visual P3 response, but with a lower magnitude effect (the effect has lowest magnitude for the non-target case).

#### Statistical analysis

The dataset consists of 45 male subjects in each control, alcoholic and high-risk groups. The control and high-risk groups are age-matched with an average age of

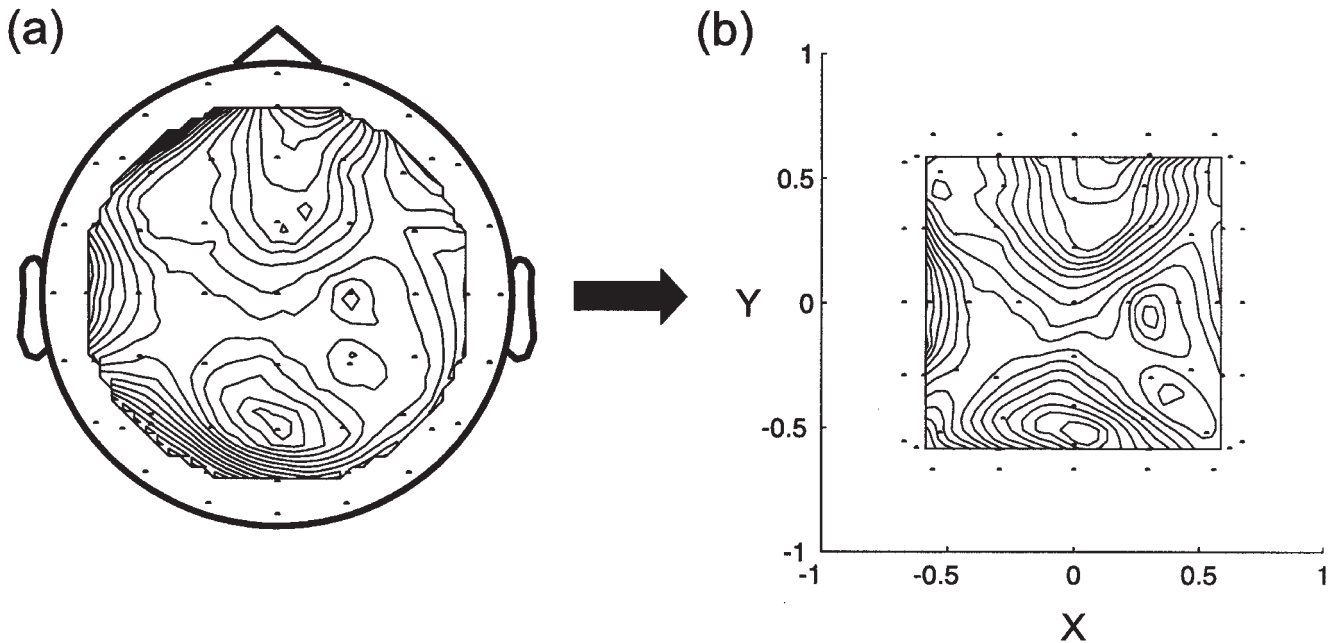


Figure 5. The surface Laplacian ERP data is transformed from spherical data slices (a) to a data square (b) to allow calculation of the wavelet packet transform decomposition tree. Note, the peripheral electrodes are cut from the dataset due to edge effects from the surface Laplacian calculation. Electrode positions are indicated by black dots.

22.2 (standard deviation  $\pm 2.6$ ) and 22.3 (standard deviation  $\pm 2.2$ ), respectively. The alcoholic group is older, with an average age of 35.5 years (standard deviation 12.1). The alcoholic group was recruited from individuals undergoing treatment in the Short Term Alcohol Treatment Unit, Addictive Disease Hospital, Kings County Hospital Center, New York. The control and high-risk groups were individuals who responded to advertisements and postings at the SUNY Health Science Center. The subjects were required to provide details regarding alcohol and drug use, and medical and psychiatric histories.

Principal component analysis (PCA) was performed on the complexity curves (e.g., figure 6c) for each of the three stimulus cases and each subject. Each principal component is a linear combination of the original variables and is orthogonal to one another so there is no redundant information. Commonly, the sum of the variances of the first few principal components will characterize the majority of the total variance of the original data; hence, multi-valued problems may be represented with a few variables.

In the following analysis the largest principal component was used to test for statistically significant differences among groups. The results of the analysis are depicted in the box and whisker displays of figure 7. Significant t-test  $p$ -values are observed between the control and alcoholic subjects for the target case ( $p$ -value  $< 0.003$ ) and novel case ( $p$ -value  $< 0.038$ ); and between the control

and high-risk groups for the target case ( $p$ -value  $< 0.012$ ). Visual inspection of the complexity curves, in which we observe significant differences, reveals that complexity values for the control subjects are on average lower than the high-risk and alcoholic subjects during and after the visual P3 component.

The previous statistical analysis is based on the assumption that the data is normally distributed. However, using a non-parametric approach for significance testing allows the replacement of formal assumptions with a more computationally intensive approach through "permutation" tests. Given the null hypothesis that the labeling of the groups is arbitrary, then the significance of a statistic expressing group differences can be assessed by comparison with the distribution of values obtained by random permutation of the labels (Holmes et al. 1996). If there are no differences between groups, then a statistic value produced by any other re-labeling (permutation) of the data is as likely as the true labeling. By considering all re-labelings of the data (or an appropriately high number), a  $p$ -value can be computed for the chosen statistic.

In general, any statistic can be used for the non-parametric analysis; here we use the following t-statistic, essentially a mean difference normalized by a variance estimate:

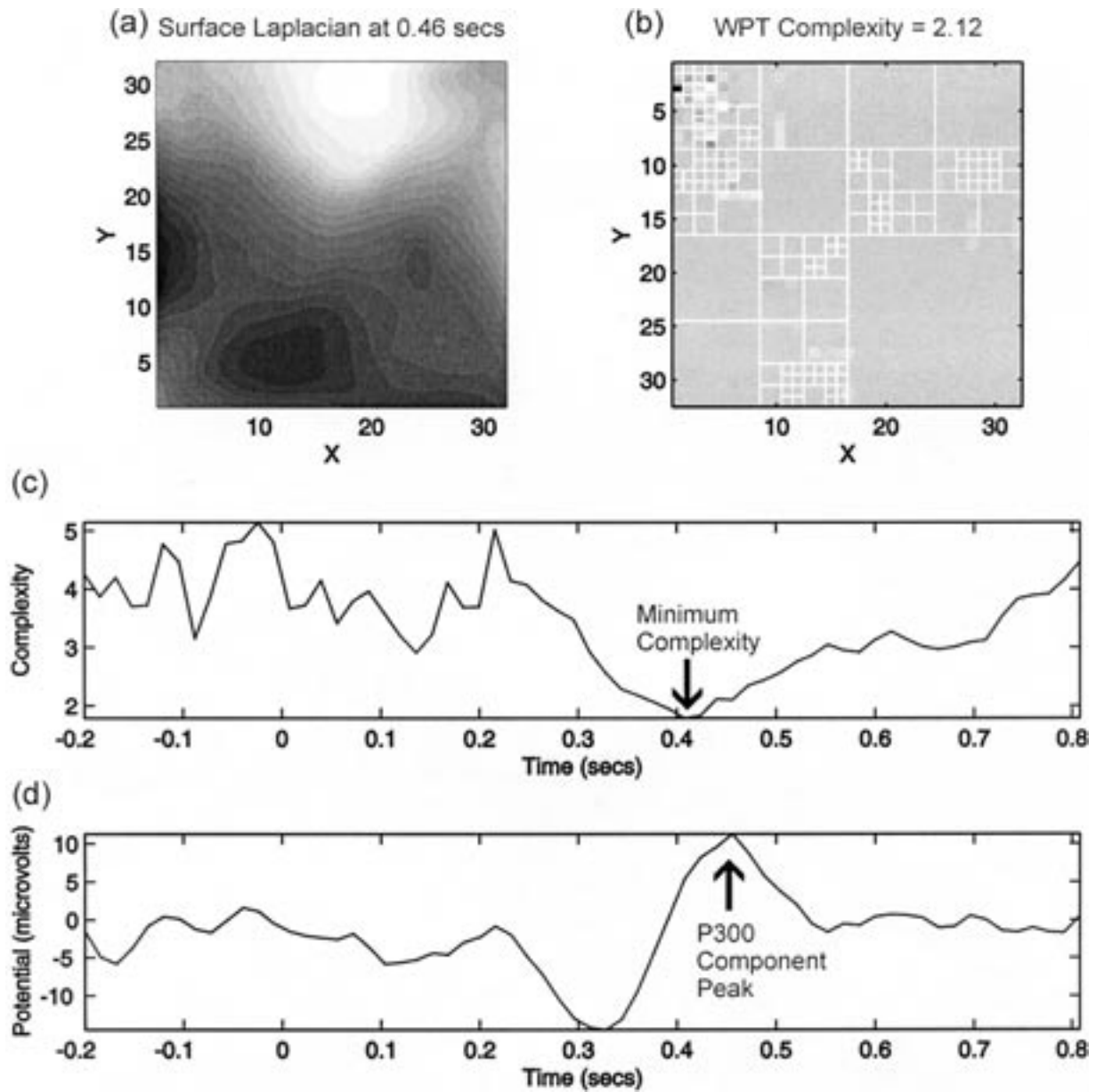


Figure 6. Example of a complexity curve calculated from 45 male control subject Visual Oddball target case data. Plot (a) is the mean surface Laplacian transformed ERP data at 460 ms following stimulus onset. The best-basis wavelet decomposition of image (a) is shown in (b), with phase-planes plotted in white; the relative complexity of image (a) is calculated as 2.12. Plot (c) shows the curve of complexity values (averaged) calculated from 200 ms pre stimulus onset to 800 ms post-stimulus onset. For comparison, the corresponding mean brain potential is plotted in (d) for electrode CZ.

$$t = \frac{(\bar{x}_1 - \bar{x}_2)}{\sqrt{\frac{S_p^2}{n_1} + \frac{S_p^2}{n_2}}}$$

where  $\bar{x}_1$  and  $\bar{x}_2$  are the means of group 1 and group 2,  $n_1$  and  $n_2$  are the sample sizes of group 1 and group 2. The pooled variance,  $S_p^2$  is calculated by:

$$S_p^2 = \frac{SS_1 + SS_2}{(n_1 - 1) + (n_2 - 1)},$$

where  $SS_1$  and  $SS_2$  are the sums of squares of group 1 and group 2, respectively. This t-statistic is computed for each possible data re-labeling  $i = 1, \dots, N$ , or for a high number of permutations (e.g.,  $N = 1000$ ), giving  $t_i$ . The critical threshold value,  $T_c$ , for a significance level of  $\alpha$  is the  $c + 1$  largest

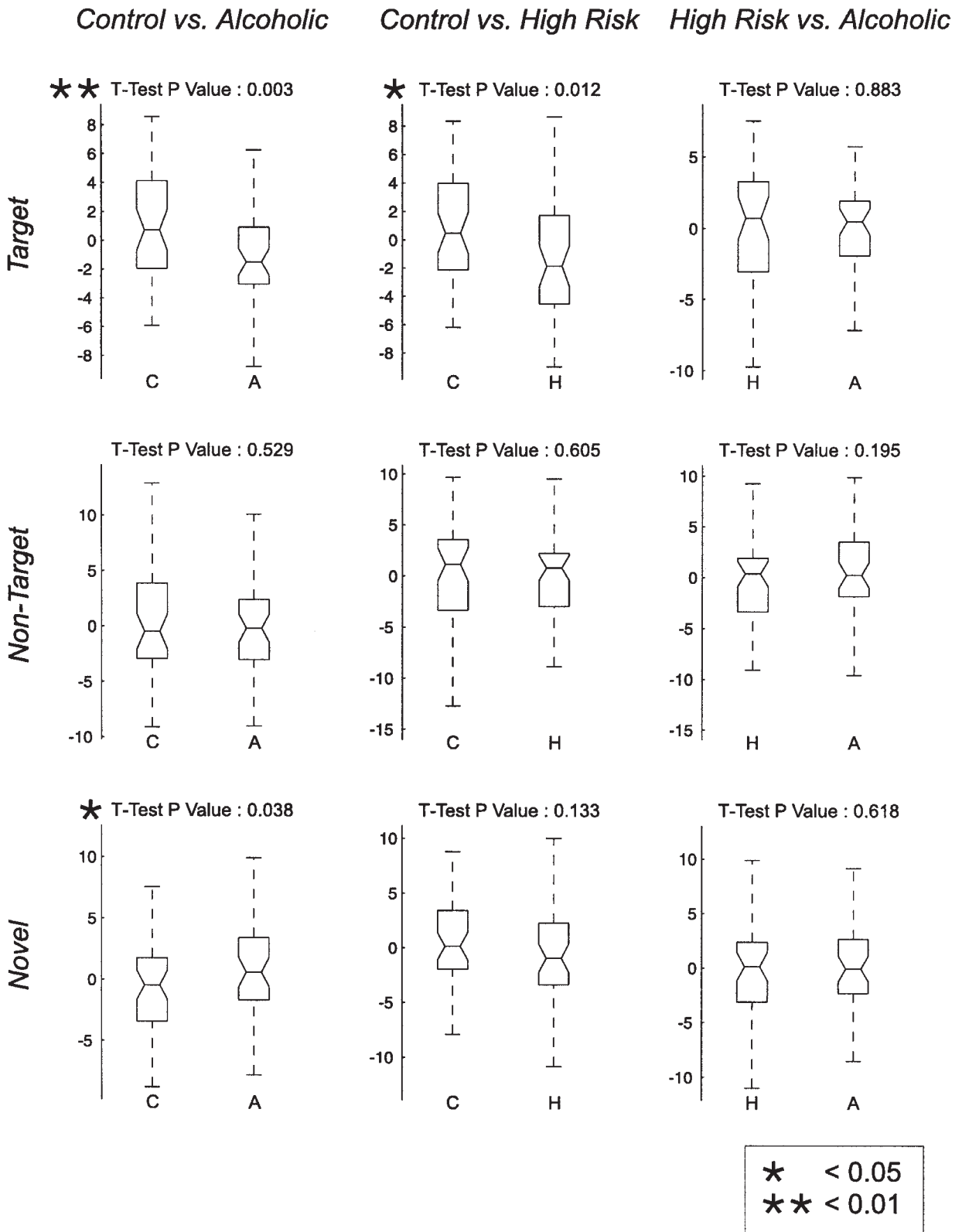


Figure 7. Box and whisker plots of the largest principal component for control vs. alcoholic, control vs. high-risk, and high-risk vs. alcoholic groups; and target, non-target and novel cases. The t-test  $p$ -values indicate significant differences for the control and alcoholic group data for the target and novel cases ( $p$ -value less than 0.01 and less than 0.05, respectively), and a significant difference between the control and alcoholic group for the novel case ( $p$ -value less than 0.05).

Table I. Summary of significant results of parametric and non-parametric tests calculated on the largest principal component of the spatial complexity curves. When the t-statistic value exceeds the critical threshold values  $T_c$  (estimated by permutation) then the group differences are significant (indicated in bold) at the threshold significance level  $\alpha$ . The non-parametric results confirm the  $p$ -values given by a student's t-test (\* <0.05, \*\* <0.01).

	<i>p</i> -value	t-statistic	$T_c$ ( $\alpha = 0.05$ )	$T_c$ ( $\alpha = 0.01$ )
Control vs. Alcoholic (target)	0.002**	2.966	<b>2.045</b>	<b>2.558</b>
Control vs. Alcoholic (novel)	0.038*	2.066	<b>1.965</b>	2.563
Control vs. High Risk (target)	0.012*	2.478	<b>1.920</b>	2.585

member of  $t_i$ , where  $c = \lambda\alpha N\mu$ . If the t-statistic for the correctly labeled data exceeds the threshold value, then the null hypothesis can be rejected and differences are significant at the level of  $\alpha$  (i.e., 0.05 or 0.01).

Table I presents a summary of the significant parametric and non-parametric results. Critical threshold values ( $T_c$ ) shown in bold are less than the t-statistic value and so indicate a significant result at the specified significance level  $\alpha$ . Clearly, the non-parametric results show good agreement with the more traditional parametric t-test results. If the assumptions regarding the parametric statistical analysis are in doubt, then the result of a non-parametric method will provide the only guaranteed result. However, if the assumptions of the parametric method are true, then the result of the non-parametric method provides a validation of these results.

## Discussion and Conclusions

We have presented in this paper a method, based on the 2-D wavelet packet transform with best-basis algorithm, to derive an estimate of the spatial complexity of brain activity for event-related potential electroencephalogram recordings. The measure may be calculated at successive time-intervals for both individual trial data and case-dependent average data, provided a spatial map of brain potential or surface Laplacian data can be generated (i.e., multi-channel EEG recording), so as to provide a time-varying curve of complexity. Alternatively, temporal complexity could be calculated using the 1-D wavelet packet transform, or spatio-temporal complexity through a combination of 1-D and 2-D algorithms. The heart of the method is essentially a linear algorithm to obtain maximal sparsity which provides an estimate of the

signal entropy. Although there are a number of alternative methods which exist to calculate this measure the wavelet packet transform offers some advantages:

1. Is adaptive, and so automatically finds a transform which provides the best average compression for the signal.
2. Yields a family of orthonormal basis allowing the use of an additive cost function.
3. Allows for fast computation of  $O(N \log N)$
4. Extendable to two dimensions and higher.

However, due to the dependence of the measure upon the calculation method, and the need to select a particular orthogonal wavelet basis, the measure is relative and can only be compared with other values calculated with the same algorithm and parameters.

Application of the method to case-averaged Visual Oddball ERP data shows a decrease in spatial complexity values following the onset of the target case stimulus, and during the occurrence of the Visual P3 event; this decrease may reflect higher regional synchrony of electrical activity between channels. Decreases in spatial and temporal signal complexity have been observed in EEG data shortly after the onset of an epileptic seizure (Pijn et al. 1997; Franaszczuk and Bergey 1999; Bergey and Franaszczuk 2001). Lehenertz and Elgar (1995) suggest that signal complexity may reflect the intricacy of neuronal interactions; the observed activity has been associated with higher regional and temporal synchrony reflected in regular, rhythmic activity near the onset of a seizure. Nunez et al. (2001) summarizes findings of authors describing robust increases in measures of EEG coherence and synchrony during task performance. In general, such increases may be associated with decreases in signal entropy or complexity. Similarly, we suspect the observed decrease in spatial complexity in the Visual

Oddball experiment is due to increased spatial synchronicity of brain activity, and hence, a more predictable spatial brain pattern caused by processes associated with the event-related visual task.

The observed differences in the control vs. alcoholic and high-risk group complexity curves may be due to a physiological difference between groups. Begleiter and Porjesz (1999) propose a model for the predisposition toward alcoholism in which the CNS hyperexcitability reflects an imbalance between excitation and inhibition and that the decreased Visual P3 component amplitude in alcoholics and individuals at risk is caused by a general state of CNS disinhibition with an excess of CNS excitation. The reduced complexity values observed in this study, for the target case between the control subject group when compared to the alcoholic and high-risk groups (as indicated by the PCA analysis), may be due to these latter groups having increased CNS excitation which is reflected in decreased spatial synchronicity of neuronal firing and therefore increased spatial complexity. This possibility warrants further investigation and possible use of the measure for genetic analysis.

## Appendix

Mapping of surface Laplacian data from scalp surface to square is achieved through:

$$(x, y) \text{ a } (u, v), \text{ if } y > |x|,$$

where

$$\begin{aligned} u &= x, \\ v &= \frac{r_3}{r_1} r_2 + |x|, \\ r_1 &= \sqrt{r_2 - x_2}, \\ r_2 &= y - |x|, \\ r_3 &= \frac{\sqrt{2}}{2} r - |x|, \end{aligned}$$

and  $r$  is the radius of the scalp surface. Mapping of the regions  $-y > *x*$ ,  $x > *y*$  and  $-x > *y*$  is calculated similarly using symmetry (Wang et al. 1998).

## References

- Andino, S.L.G., De Peralta Menendez, R.G., Thut, G., Spinelli, L., Blanke, O., Michel, C.M., Seeck, M. and Landis, T. Measuring the complexity of time series: an application to neurophysiological signals. *Human Brain Mapping*, 2000, 11(1): 46-57.
- Baraniuk, R.G., Flandrin, P., Hansen, A.J.E.M. and Micheal, O. Measuring Time Frequency Information Content using Rényi Entropies. 1998, Available at <http://www-dsp.rice.edu/publications>.
- Begleiter, H., Porjesz, B. What is inherited in the predisposition of alcoholism? A proposed model. *Alcohol Clin. Exp. Res.*, 1999, 23: 1125-1135.
- Begleiter, H., Porjesz, B., Bihari, B. and Kissin, B. Event-related potentials in boys at high risk for alcoholism. *Science*, 1984, 225: 1493-1496.
- Benegal, V., Jain, S., Subbukrishna, D.K. and Channabasavanna, S.M. P300 amplitudes vary inversely with continuum of risk in first degree male relatives of alcoholics. *Psychiatr. Genet.*, 1995, 5: 1-8.
- Bergey, G.K. and Franaszczuk, P.J. Epileptic Seizures are characterized by changing signal complexity. *Clinical Neurophysiology*, 2001, 112: 241-249.
- Berman, M.S., Whipple, S.C., Fitch, R.J. and Noble, E.P. P3 in young boys as a predictor of adolescents' substance abuse. *Alcohol*, 1993, 10: 69-76.
- Bhattacharya, J. Complexity analysis of spontaneous EEG. *Acta. Neurobiol. Exp.*, 2000, 60: 495-501.
- Cohen, H.L., Wang, W., Porjesz, B. and Begleiter, H. Auditory P300 in young alcoholics: regional response characteristics. *Alcohol Clin. Exp. Res.*, 1995, 19: 469-475.
- Coifman, R.R. and Meyer, Y. Orthonormal Wave Packet Bases. Technical Report, Yale Univ., New Haven, CT, August 1989.
- Coifman, R.R. and Wickerhauser, M.V. Best Adapted Wavelet Packets Bases. Technical Report, Yale Univ., New Haven, CT, February 1990.
- Coifman, R.R. and Wickerhauser, M.V. Entropy based algorithms for best basis selection. *IEEE Trans. Inform. Theory*, 1992, 38(2): 713-718.
- Emmerson, R.Y., Dustman, R.E., Shearer, D.E. and Chamberlin, H.M. Visually evoked and event related potentials in young abstinent alcoholics. *Alcohol*, 1987, 4: 241-248.
- Feldman, D. Information Theory, Excess Entropy and Statistical Complexity: Discovering and Quantifying Statistical Structure. Technical Report, 1998. Available at <http://hornacek.coa.edu/dave/Tutorial>.
- Fell, J., Röschke, J., Mann, K. and Schäffner, C. Discrimination of sleep stages: a comparison between spectral and nonlinear EEG Measures. *Electroenceph. and Clin. Neurophysiol.*, 1996, 98: 401-410.
- Franaszczuk, P.J. and Bergey, G.K. An Autoregressive method for the measurement of synchronization of interictal and ictal EEG signals. *Biol. Cybern.*, 1999, 81: 3-9.
- Grassberger, P. and Procaccia, I. Measuring the Strangeness of strange attractors. *Physica D*, 1983, 9D: 189-208.
- Hill, S.Y. and Steinhauser, S.R. Assessment of Prepubertal and postpubertal boys and girls at risk for developing alcoholism with p300 from a visual discrimination task. *J. Stud. Alcohol*, 1993, 54: 350-358.
- Holmes, A.P., Blair, R.C., Watson, J.D.G. and Ford, I. Nonparametric Analysis of statistic images from functional mapping experiments. *Journal of Cerebral Blood Flow and Metabolism*, 1996, 16(1): 7-22.
- Jasper, H.H. The ten-twenty electrode system of the international federation. *Electroencephalogr. Clin. Neurophysiol.*, 1958, 10: 371-375.

- Jeong, J., Gore, J.C. and Peterson, P.S. Mutual Information analysis of the EEG in patients with alzheimer's disease. *Clin. Neurophysiol.*, 2001, 112: 827-835.
- Katznelson, R.D. EEG Recording Electrode Placement, and Aspects of Generator Localization. In: P.L. Nunez (Ed.), *Electric Fields of the Brain: The Neurophysics of EEG*. Oxford University Press, New York, 1981.
- Kolmogorov, A.N. Three approaches to the quantitative definition of information. *Problems of Information Transmission*, 1965, 1(1): 1-17.
- Le, J., Menon, V. and Gevins, A. Local estimate of surface laplacian derivation on a realistically shaped scalp surface and its performance on noisy data. *Electroenceph. and Clin. Neurophysiol.*, 1994, 92: 433-441.
- Lehertz, K. and Elgar, C.E. Spatio-temporal dynamics of the primary epileptogenic area in temporal lobe epilepsy characterized by neuronal complexity loss. *Electroenceph. Clin. Neurophysiol.*, 1995, 95: 108-117.
- Lloyd, S. Use of mutual information to decrease entropy: implications for the second law of thermodynamics. *Phys. Rev. A*, 1989, 39(10): 5378-5386.
- Nunez, P.L. *Neocortical Dynamics and Human EEG Rhythms*. Oxford University Press, New York, 1995.
- Nunez, P.L., Silberstein, R.B., Cadusch, P.J., Wijesinghe, R.S., Westrop, A.F. and Srinivasan, R.A. A theoretical and experimental study of high resolution EEG based on surface laplacians and cortical imaging. *Electroenceph. and Clin. Neurophysiol.*, 1994, 90: 40-57.
- Nunez, P.L., Wingeier, B.M. and Silberstein, R.B. Spatial-temporal structures of human alpha rhythms: theory, microcurrent sources, multiscale measurements, and global binding of local networks. *Human Brain Mapping*, 2001, 13: 125-164.
- Olshausen, B.A. and Field, D.J. Natural image statistics and efficient coding. *Network*, 1996, 7: 333-339.
- Patterson, B.W., Williams, H.L., McLean, G.A., Smith, L.T. and Schaffer, K.W. Alcoholism and family history of alcoholism: effects on visual and auditory event-related potentials. *Alcohol*, 1987, 4: 265-274.
- Pezard, L., Martinerie, J., Müller, J., Varela, F. and Renault, B. multichannel measures of average and localized entropy. *Physica D*, 1996, 96: 344-354.
- Pfefferbaum, A., Ford, J.M., White, P.M. and Mathalon, D. Event-related potentials in alcoholic men: p3 amplitude reflects family history but not alcohol consumption. *Alcohol Clin. Exp. Res.*, 1991, 21: 521-529.
- Pijn, J.P., Velis, D.N., van der Heyden, M.J., DeGoede, J., van Veelan, C.W. and Lopes da Silva, F.H. Non-linear dynamics of epileptic seizures on basis of intracranial EEG recordings. *Brain Topography*, 1997, 9: 249-270.
- Pincus, S.M. Approximate entropy as a measure of system complexity. *Proc. Natl. Acad. Sci. USA*, 1991, 88: 2297-2301.
- Porjesz, B., Begleiter, H., Bihari, B. and Kissin, B. Event-related brain potentials to high incentive stimuli in abstinent alcoholics. *Alcohol*, 1987, 4: 283-287.
- Porjesz, B., Begleiter, H. and Garrozo, R. Visual Evoked Potential Correlates of Information Processing Deficits in Chronic Alcoholics. In: H. Begleiter (Ed.), *Biological Effects of Alcohol*. Plenum, New York, 1980: 603-623.
- Rényi, A. On measures of entropy and information. *Proceedings of the 4th Berkeley Symposium on Mathematics, Statistics and Probability*, 1960: 547-561.
- Rezek, I.A. and Roberts, S.J. Stochastic Complexity Measures for Physiological Signal Analysis. Technical report, Imperial College, University of London, November 1998. Available at <http://www.ee.ic.ac.uk/hp/staff/sroberts.html>.
- Roberts, S., Penny, W. and Rezek, I. Temporal and spatial complexity measures for eeg-based brain-computer interfacing. *Medical and Biolog. Eng. and Comput.*, 1998, 37(1): 93-99.
- Shannon, C.E. A mathematical theory of communication. Part I, *Bell Sys. Tech. J.*, 1948, 27: 379-423.
- Shannon, C.E. and Weaver, W. *Mathematical Theory of Communication*. Urbana: University of Illinois Press, 1964.
- Srinivasan, R., Nunez, P. and Silberstein, R. Spatial filtering and neocortical dynamics: estimation of EEG coherence. *IEEE Trans. Biomed. Eng.*, 1998, 48: 814-826.
- Takens, F. Detecting Strange Attractors in Turbulence. In: D.A. Rand and L.S. Young (Eds.), *Dynamical Systems and Turbulence*. Berlin, Springer, 1981: 366-381.
- Trgo, A. and Wickerhauser, M.V. A Relation Between Shannon-Weaver Entropy and "Theoretical Dimension" for Classes of Smooth functions. Preprint, 1996. Available at <http://www.math.wustl.edu/~victor/papers>.
- van der Stelt, O., Geesken, R., Gunning, W.B., Snel, J. and Kok, A. P3 scalp topography to target and novel stimuli in children of alcoholics. *Alcohol*, 1998, 15: 119-136.
- Wang, K. and Begleiter, H. Local polynomial estimate of surface laplacian. *Brain Topography*, 1999, 12: 19-29.
- Wang, K., Begleiter, H. and Porjesz, B. Spatial enhancement of event-related potentials using multiresolution analysis. *Brain Topography*, 1998, 10: 191-200.
- Weber, B., Lehnertz, K., Elgar, C.E. and Weiser, H.G. Neuronal complexity loss in interictal EEG recorded with foramen ovale electrodes predicts side of primary epileptogenic area in temporal lobe epilepsy: a replication study. *Epilepsia*, 1998, 39: 922-927.
- Whipple, S.C., Berman, S.M. and Noble, E.P. Event related potentials in alcoholic fathers and their sons. *J. Stud. Alcohol*, 1991, 8: 321-327.
- Whipple, S.C., Parker, E.S. and Noble, E.P. An atypical neurocognitive profile in alcoholic fathers and their sons. *J. Stud. Alcohol*, 1988, 49: 240-244.
- Wolf, A., Swift, J.B., Swinney, L. and Vastano, J.A. Determining lyapunov exponents from a time series. *Physica D*, 1985, 16: 285-317.